

Planetary Nebulae and Their Central Stars in the X-ray and EUV Regions

Martín A. Guerrero

Instituto de Astrofísica de Andalucía, IAA-CSIC,
Camino Bajo de Huétor, 50, E-18008 Granada, Spain
email: mar@iaa.es

Abstract. *Einstein*, *EXOSAT*, and *ROSAT* X-ray observations of planetary nebulae detected soft photospheric X-ray emission from their central stars, but the diffuse X-ray emission from the shocked fast stellar wind in their interiors could not be unambiguously resolved. The new generation of X-ray observatories, *Chandra* and *XMM-Newton*, have finally resolved the diffuse X-ray emission from shocked fast winds in planetary nebula interiors. Furthermore, these observatories have detected diffuse X-ray emission from bow-shocks of fast collimated outflows impinging on the nebular envelopes, and unexpected hard X-ray point-sources associated with the central stars of planetary nebulae. Here I review the results of these new X-ray observations of planetary nebulae and discuss the promise of future observations.

Keywords. planetary nebulae: general

1. Introduction: X-ray Emission from Planetary Nebulae

X-ray emission is produced by hot gas at temperatures greater than 10^6 K. Therefore, the detection of X-ray emission reveals energetic phenomena involving high temperatures, strong collisions or accretion. In planetary nebulae (PNe), there are different mechanisms that can produce weak, but detectable X-ray emission:

- Photospheric emission from the hot central star

The photospheric emission of hot, $>100,000$ K, central stars of PNe can have high-energy tails extending into the X-ray domain. The photospheric X-ray emission from the central stars of PNe will produce point-sources of soft X-ray emission, peaking below ~ 0.2 keV.

- Coronal emission from a dwarf companion

A hard and variable X-ray point-source at the central star of a PN can reveal the coronal emission from a dwarf companion. This X-ray emission may be powered by the orbital coupling between the central star of the PN and the dwarf companion.

- Shocked fast stellar wind

In the standard interacting-stellar-winds model of PN formation, the fast stellar wind emanating from the central star sweeps up the slow wind of the Asymptotic Giant Branch (AGB) phase to form a sharp nebular shell. This central cavity is expected to be filled with shock-heated fast wind that emits X-rays with a limb-brightened morphology.

- Fast collimated outflows

Fast collimated outflows that occur near the end of the AGB phase impinge on the AGB wind, producing bow-shock structures. When the shock velocity is >300 km s $^{-1}$, extended cavities filled with hot X-ray-emitting gas can be formed.

X-ray observations of a point-source associated with the central star of a PN can be used to study the late stellar evolution and to unveil a hidden companion that has escaped detection so far. Furthermore, the processes responsible of the production of diffuse hot gas in a PN are closely tied to the shaping of the PN itself. X-ray observations of PNe are

key to assessing the action of fast stellar winds and collimated outflows in the formation and evolution of PNe.

2. X-ray Point-Sources at the Central Stars of Planetary Nebulae

The detections of X-ray point-sources at the central stars of PNe have shown a large variety of spectral properties and luminosity levels. Several emission mechanisms are responsible for the different types of observed X-ray point-sources in PNe.

2.1. Photospheric X-ray Emission

Einstein, *EXOSAT*, and *ROSAT* produced detections of soft X-rays associated with the photospheric emission of the central stars of A 36, K 1-16, K 1-27, LoTr 5, NGC 246, NGC 1360, NGC 3587, NGC 4361, NGC 6853, and NGC 7293 (de Korte *et al.* 1985; Tarafdar & Apparao 1988; Apparao & Tarafdar 1989; Kreysing *et al.* 1992; Rauch, Koepfen & Werner 1994; Hoare *et al.* 1996). Our analysis of all X-ray observations of PNe in the entire *ROSAT* archive (Guerrero, Chu, & Gruendl 2000) concluded that distance, extinction, and evolutionary status are critical for the detection of the photospheric emission from hot central stars of PNe. Since the absorption cross sections for the soft photospheric emission from the central stars of PNe are large, only the hot central stars of nearby, large, tenuous, evolved PNe with small absorption column densities of intervening material are detected.

Further studies of the photospheric X-ray emission from central stars of PNe are difficult. The *Chandra* LETG and *XMM-Newton* RGS can provide high-dispersion spectra in the 10–200 Å wavelength range, but the sensitivity of both instruments at low energies is really low.

2.2. Coronal Emission from a Dwarf Companion

ROSAT PSPC observations of LoTr 5 and NGC 7293 detected a hard (>0.5 keV) X-ray component at the central stars of these PNe that cannot be attributed to photospheric emission (Kreysing *et al.* 1992; Leahy, Zhang, & Kwok 1994). LoTr 5 is a known binary (perhaps even triple) system (Jasniewicz *et al.* 1996), and so the hard X-ray component can be attributed to coronal emission from the G companion of the central star. NGC 7293 is not a known binary, but the spatial and spectral properties and the variability of the hard X-ray emission are consistent with the X-ray emission from a quiescent dMe companion (Guerrero *et al.* 2001). This conclusion is supported by the observed variability in the stellar H α and [N II] emission (Gruendl *et al.* 2001). Recent *Spitzer* observations, however, have failed to detect any sign of the dwarf companion at 3.6, 4.5, 5.8, and 8.0 μm . Instead, these observations have discovered 24 and 70 μm emission at the central star of NGC 7293 that can be associated with a cold, ~ 100 K, source.

2.3. Shocks in Winds?

Chandra observations of NGC 6543 detected a hard point-source at its central star (Chu *et al.* 2001). The spectral properties of this source discounts photospheric emission from the central star of NGC 6543, while the presence of a dwarf companion is uncertain (Guerrero *et al.* 2001). The fast stellar wind of the central star of NGC 6543 is known to be variable (Méndez, Herrero, & Manchado 1990) and the X-ray to bolometric luminosity ratio of the central star X-ray source is $L_X/L_{\text{bol}} \sim 10^{-7}$, as observed in O stars (Sana, Rauw, & Gosset 2005). Therefore, it can be speculated that instabilities in the stellar wind of NGC 6543 create shocks that produce X-ray-emitting gas.

2.4. Other Detections of Hard Point-Sources

Other hard point-sources detected at the central stars of PNe can be attributed to different mechanisms. For instance, *Chandra* has detected an obscured and presumably hard X-ray source associated with the central star of Mz 3, a bipolar nebula around a possible symbiotic star (Kastner *et al.* 2003). The X-ray emission from this point-source may be explained by the coronal activity of a dwarf companion, but a magnetized accretion disk has also been invoked based on the possible detection in Mz 3 of an X-ray jet.

In K 3-35, *XMM-Newton* observations have marginally detected a source at its center. This X-ray source can be attributed to a dwarf companion, to diffuse emission unresolved by *XMM-Newton*, or even to a field star. However, since K 3-35 is an extremely young PN with a magnetized toroidal structure probably collimating fast outflows (Miranda *et al.* 2001), it is tantalizing to attribute the X-ray source detected by *XMM-Newton* to the residual coronal activity associated with the magnetic field generated by a stellar dynamo at the end of the AGB phase (Blackman *et al.* 2001).

Finally, inspired by the detection of hard X-ray emission from the central star of NGC 7293, O'Dwyer *et al.* (2003) and Chu *et al.* (2004) have performed a search for hard X-ray emission from white dwarfs (WDs), the descendants of the central stars of PNe. In most cases, hard X-ray emission associated with WDs could be attributed to a dwarf companion or to accretion, but the hard X-ray emission from KPD 0005+5106 and PG 1159 seems to be real. These two are among the hottest, low metal content WDs. It is possible that the observed X-ray emission from these two WDs is a leakage of the Wien high-energy tail from deep in the stellar atmosphere.

3. Diffuse X-ray Emission from Planetary Nebulae

Before the launch and operation of *Chandra* and *XMM-Newton*, *ROSAT* and *ASCA* observations of PNe provided the first indications of the diffuse X-ray emission expected from hot gas in PN interiors (Kreysing *et al.* 1992). This diffuse X-ray emission, however, was only marginally resolved (Leahy, Kwok, & Yin 2000), and the spectral analysis was very limited, apart from the *ASCA* observations of BD+30°3639 (Arnaud, Borkowski, & Harrington 1996).

3.1. *Chandra* and *XMM-Newton* Observations of Planetary Nebulae

Chandra and *XMM-Newton* provide unprecedented sensitivity and angular resolution, which make it possible to detect and resolve the diffuse X-ray emission from hot gas in PNe. Some of these observations have produced exquisite X-ray images and useful spectra, for example, BD+30°3639 (Kastner *et al.* 2000) and NGC 6543 (Chu *et al.* 2001). Figure 1 illustrates the distribution of diffuse X-ray emission relative to the nebular shell of NGC 6543. Comparisons of the X-ray contours and the H α image of this PN show that the diffuse X-ray emission is bounded by the sharp rim of the central elliptical shell and the two lobes extending along its major axis (Chu *et al.* 2001).

To date, observations made with *Chandra* and *XMM-Newton* have unambiguously resolved diffuse X-ray emission from 10 PNe and proto-PNe, as listed in Table 1. It is noticeable that a significant fraction of PNe have not been detected by sensitive *Chandra* and *XMM-Newton* observations. It is possible to explain these non-detections. Large, evolved PNe do not possess X-ray-emitting gas because the mechanical luminosity of the wind of their central stars has largely diminished and because the large volume of their central cavities implies that the hot gas in their interior has cooled significantly (e.g., NGC 3132 and NGC 4361). PNe with an open shell morphology do not have X-ray-emitting gas either, because the hot gas has blown-out in the interstellar medium (e.g.,

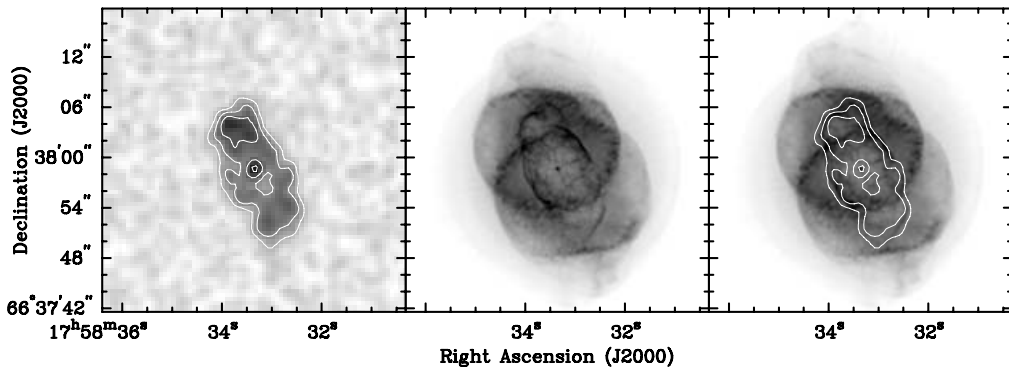


Figure 1. NGC 6543. *Left:* *Chandra* ACIS-S image in the 0.3–2.0 keV energy band. *Center:* *HST* WFPC2 H α image. *Right:* H α image overlaid by X-ray contours. Adapted from Chu *et al.* (2001).

Table 1. *Chandra* and XMM-Newton Detections of Hot Gas in Planetary Nebulae

Planetary Nebula	X-ray Observatory	Count Rate (cnts s ⁻¹)	Observed Flux (ergs cm ⁻² s ⁻¹)	Reference
BD+30° 3639	<i>Chandra</i>	0.242	6.8×10^{-13}	1
Hen 3-1475	<i>Chandra</i>	0.0015	5.1×10^{-15}	2
Mz 3	<i>Chandra</i>	0.0015	7.0×10^{-15}	3
NGC 40	<i>Chandra</i>	0.0029	1.7×10^{-14}	4
NGC 2392	XMM-Newton	0.0534	6.0×10^{-14}	5
NGC 3242	XMM-Newton	0.0384	6.7×10^{-14}	6
NGC 6543	<i>Chandra</i>	0.0316	1.0×10^{-13}	7
NGC 7009	XMM-Newton	0.0615	7.2×10^{-14}	8
NGC 7026	XMM-Newton	0.0083	8.8×10^{-15}	9
NGC 7027	<i>Chandra</i>	0.014	3.1×10^{-14}	10

References: (1) Kastner *et al.* (2000), (2) Sahai *et al.* (2003), (3) Kastner *et al.* (2003), (4) Montez *et al.* (2005), (5) Guerrero *et al.* (2005), (6) Ruiz *et al.* (these proceedings), (7) Chu *et al.* (2001), (8) Guerrero *et al.* (2002), (9) Gruendl *et al.* (2006), (10) Kastner, Vrtilik, & Soker (2001)

Hen 2-104 and NGC 2346). Finally, PNe with moderate velocity (≤ 200 km s⁻¹) collimated outflows do not show X-ray emission because the shock velocity of these outflows is not high enough to produce X-ray-emitting gas (e.g. CRL 618 and Hen 2-90).

3.2. The Origin of the Hot Gas in Planetary Nebulae

In general, diffuse X-ray emission is observed to be confined within the innermost nebular shell of young PNe with a sharp, closed shell morphology (e.g., NGC 40 and NGC 7009) or within the closed lobes of bipolar PNe (e.g., NGC 7026 and NGC 7027). The spatial distribution of X-ray emission in PNe is consistent with the expected distribution of shocked fast wind in the interacting-stellar-winds model. The only notable exception is the proto-PN Hen 3-1475, for which *Chandra* observations provide the only clear detection of X-ray emission from the bow-shock of a collimated outflow (Sahai *et al.* 2003).

Other indications that fast collimated outflows may be responsible for the production of hot gas in PNe are provided by the asymmetrical X-ray morphology typically seen in PNe (Kastner *et al.* 2002), and by the possible presence of an X-ray jet in Mz 3 (Kastner

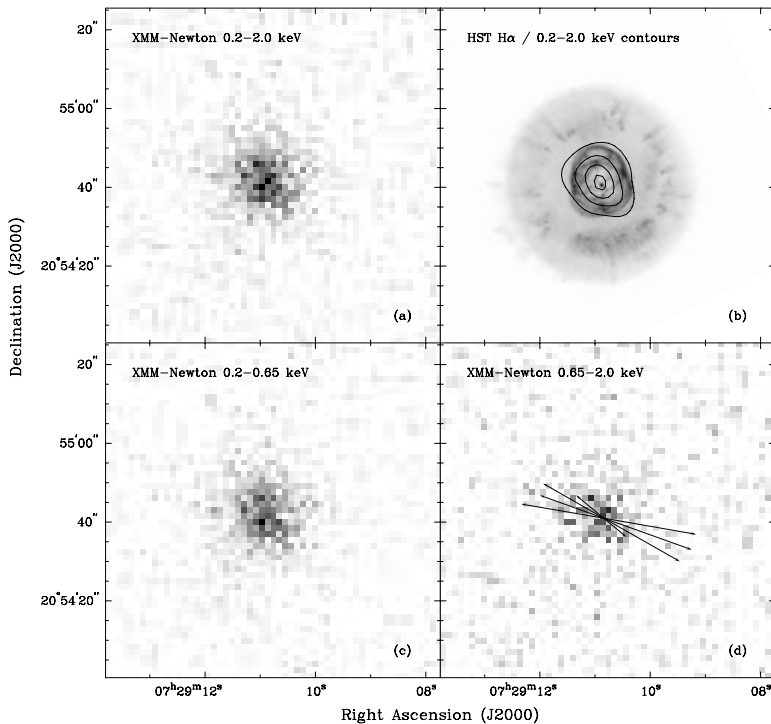


Figure 2. *XMM-Newton* and *HST* $H\alpha$ images of NGC 2392. Panel (a) displays the *XMM-Newton* EPIC raw image in the 0.2-2.0 keV band. Panel (b) shows the *HST* $H\alpha$ image overplotted by the 25%, 50%, 75%, and 95% X-ray contours extracted from the adaptively smoothed 0.2-2.0 keV band image. Panels (c) and (d) display *XMM-Newton* EPIC raw images in the 0.2-0.65 and 0.65-2.0 keV energy bands, respectively. Pixel size in these images is 1.5". The arrows in panel (d) mark the location of the fast collimated outflow as derived from high-dispersion echelle spectroscopy. Adapted from Guerrero *et al.* (2005).

et al. 2003). Further evidence is provided by the *XMM-Newton* observations of NGC 2392, that suggest that both fast stellar winds and collimated outflows may be responsible for its diffuse X-ray emission (Guerrero *et al.* 2005). NGC 2392 is known for the exceptionally large expansion velocity of its inner shell, ~ 90 km s $^{-1}$, and the existence of a fast bipolar outflow with a line-of-sight expansion velocity approaching 200 km s $^{-1}$. The diffuse X-ray emission from NGC 2392 shows different spatial distributions between the 0.2-0.65 keV and 0.65-2.0 keV bands (Figure 2). The soft X-ray emission is confined within the inner shell as expected from shocked fast wind, while the harder X-ray emission in the 0.65-2.0 keV band is roughly aligned along the fast bipolar outflow, suggesting possible production of hot gas by the interaction of the fast bipolar outflow with nebular material.

3.3. Physical Conditions of the Hot Gas in Planetary Nebulae

The X-ray spectra of the PNe with detected X-ray emission have been used by several authors to derive different physical parameters of the hot gas in PN interiors, including its X-ray luminosity, temperature, density, and thermal pressure. An example of spectral fits to several X-ray spectra of PNe is shown in Figure 3. The determination of these parameters, however, is not homogeneous, as, for instance, the spectral analyses use different calibrations of the X-ray instruments. We have undertaken a systematic analysis of X-ray emission from PNe, applying the most up-to-date calibration files and software tools provided by *Chandra* and *XMM-Newton* to X-ray observations of PNe and the

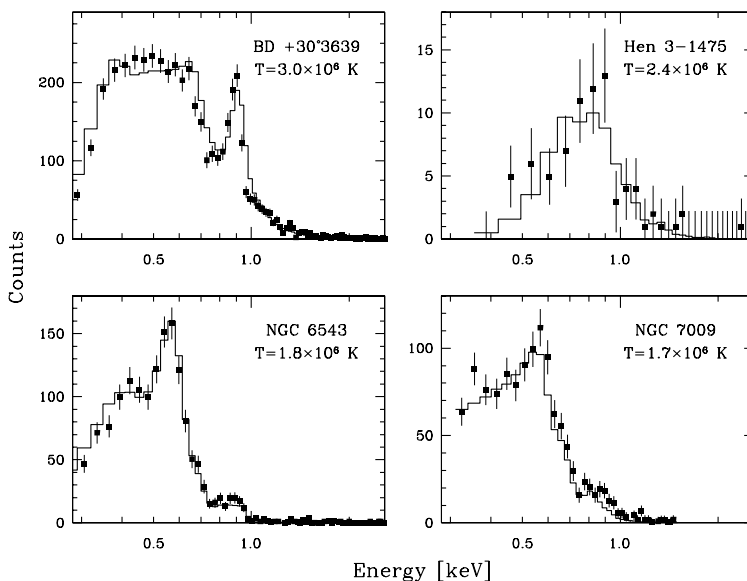


Figure 3. *Chandra* ACIS-S spectra of BD+30°3639, Hen3-1475, and NGC 6543, and *XMM-Newton* EPIC-pn spectrum of NGC 7009. The histogram overlaid on each spectrum corresponds to the best-fit model.

results are forming the XPN Database that can be accessed at <http://www.iaa.csic.es/xpn> (Guerrero, Chu, & Gruendl, these proceedings). The X-ray temperature and luminosity of PNe derived from this systematic analysis range from 1.7×10^6 K to 8×10^6 K, and from 2×10^{30} ergs s $^{-1}$ to 8×10^{32} ergs s $^{-1}$, respectively. The new results for the X-ray luminosity of NGC 2392, NGC 6543, and NGC 7009 are in close agreement with the theoretical predictions made by Schönberner, Steffen & Warmuth (these proceedings).

As cold nebular material is expected to evaporate into the hot gas and the chemical composition of the fast stellar wind and nebular material are different, the abundances of the hot gas can be used to assess the role of mass evaporation and heat conduction at the conduction layer. *Chandra* and *XMM-Newton* spectra of PNe have been used to estimate the chemical composition of the hot gas in PNe, but the results of these estimates are not conclusive (e.g. Maness *et al.* 2003). This is partially due to the limited spectral resolution of the X-ray CCD spectroscopic observations of PNe that does not allow but a crude determination of the chemical abundances of the hot gas. The better spectral resolution and coverage provided by the CCDs on-board of *Suzaku* and the unprecedented spectral resolution of *Chandra* LETG and *XMM-Newton* RGS will allow a reliable determination of the chemical abundances of the hot gas in PNe (Kokubun *et al.*, these proceedings; Kastner *et al.*, these proceedings).

4. Far UV Observations of PNe

To understand the production and evolution of hot gas in PNe, it is necessary to study the physics at the conduction layer between the hot gas in the PN interior and the cool nebular shell. The hot interior gas and the cool nebular shell form a contact discontinuity where heat conduction (Spitzer 1962) is expected to occur. The resulting mass evaporation from the dense nebular shell into the hot interior lowers the temperature and raises the density of the hot gas, significantly increasing the X-ray emissivity (Schönberner

et al., these proceedings). Thermal conduction has been assumed in theoretical models but not constrained empirically through observation because interfaces at a few $\times 10^5$ K require difficult UV observations. Traditionally interfaces are studied using spectral lines of C IV, N V, and O VI; however, these species can be photoionized by hot stars (especially PN central stars with effective temperatures $>100,000$ K) and the detection of these narrow absorption lines can be hampered by the stellar P Cygni profile and confused by interstellar absorption lines.

The interface layer in NGC 6543 can be studied using O VI emission because the physical properties of its interior hot gas have been established by *Chandra* observations (Chu *et al.* 2001) and its central star is too cool to produce O VI by photoionization ($T_{\text{eff}} \sim 50,000$ K, Zweigle *et al.* 1997). *Far Ultraviolet Spectroscopic Explorer (FUSE)* observations of NGC 6543 have indeed detected O VI emission. By assuming pressure balance between the hot interior gas and the conduction layer, we find that the O VI emission is consistent with the level of X-ray emission (Gruendl, Chu, & Guerrero 2004), but only if heat conduction at the interface is significantly smaller than the canonical value. Other PNe (e.g. NGC 2392 or NGC 7009) can be studied to validate the generality of this result.

5. Conclusions

In addition to previous detections of photospheric emission from hot central stars of PNe, *Chandra* and *XMM-Newton*, observations of PNe have detected hard X-ray point-sources at the central stars of PNe, as well as diffuse X-ray emission from hot gas in their central cavities and from bow-shocks associated with fast collimated outflows. The emerging picture is that young PNe with a sharp shell morphology contain significant amounts of hot gas in their interiors, but that the temperature and X-ray luminosity of this hot gas declines rapidly. On the other hand, only outflows faster than ~ 300 km s $^{-1}$ are capable to produce post-shock gas at temperatures greater than 10^6 K that can produce detectable X-ray emission.

Acknowledgements

M. A. G. is supported by MEC under grant numbers PNAYA 2002-00376 and PNAYA 2005-01495.

References

- Arnaud, K., Borkowski, K. J., & Harrington, J. P. 1996, *ApJ*, 462, L75
 Apparao, K. M. V., & Tarafdar, S. P. 1989, *ApJ*, 344, 826
 Blackman, E. G., Frank, A., Markiel, J. A., Thomas, J. H., & Van Horn, H. M. 2001, *Nature*, 409, 485
 Chu, Y.-H., Guerrero, M. A., Gruendl, R. A., Williams, R. M., & Kaler, J. B. 2001, *ApJ*, 553, L69
 Chu, Y.-H., Guerrero, M. A., Gruendl, R. A., & Webbink, R. F. 2004, *AJ*, 127, 477
 de Korte, P. A. J., Claas, J. J., Jansen, F. A., & McKechnie, S. P. 1985, *AdSpR*, 5, 57
 Gruendl, R. A., Chu, Y.-H., & Guerrero, M. A. 2004, *ApJ*, 617, L127
 Gruendl, R. A., Chu, Y.-H., O'Dwyer, I. J., & Guerrero, M. A. 2001, *AJ*, 122, 308
 Gruendl, R. A., Guerrero, M. A., Chu, Y.-H., & Williams, R. M. 2006, submitted to *ApJ*
 Guerrero, M. A., Chu, Y.-H., & Gruendl, R. A. 2000, *ApJS*, 129, 295
 Guerrero, M. A., Chu, Y.-H., Gruendl, R. A., & Meixner, M. 2005, *A&A*, 430, L69
 Guerrero, M. A., Chu, Y.-H., Gruendl, R. A., Williams, R. M., & Kaler, J. B. 2001, *ApJ*, 553, L55

- Guerrero, M. A., Gruendl, R. A., & Chu, Y.-H. 2002, *A&A*, 387, L1
- Hoare, M. G., Martin, A. B., Werner, K., & Fleming, T. 1995, *MNRAS*, 273, 812
- Jasniewicz, G., Thévenin, F., Monier, R., & Skiff, B. A. 1996, *A&A*, 307, 200
- Kastner, J. H., Balick, B., Blackman, E. G., Frank, A., Soker, N., Vrřilek, S. D., & Li, J. 2003, *ApJ*, 591, L37
- Kastner, J. H., Li, J., Vrřilek, S. D., Gatley, I., Merrill, K. M., & Soker, N. 2002, *ApJ*, 581, 1225
- Kastner, J. H., Soker, N., Vrřilek, S. D., & Dgani, R. 2000, *ApJ*, 545, L57
- Kastner, J. H., Vrřilek, S. D., & Soker, N. 2001, *ApJ*, 550, L189
- Kreysing, H. C., Diesch, C., Zweigle, J., Staubert, R., Grewing, M., & Hasinger, G. 1992, *A&A*, 264, 623
- Leahy, D. A., Kwok, S., & Yin, D. 2000, *ApJ*, 540, 442
- Leahy, D. A., Zhang, C. Y., & Kwok, S. 1994, *ApJ*, 422, L205
- Maness, H.L., Vrřilek, S.D., Kastner, J.H., & Soker, N. 2003, *ApJ*, 589, 439
- Méndez, R. H., Herrero, A., & Machado, A. 1990, *A&A*, 229, 152
- Miranda, L. F., Gómez, Y., Anglada, G., & Torrelles, J. M. 2001, *Nature*, 414, 284
- Montez, R. J., Kastner, J. H., De Marco, O., & Soker, N. 2005, *ApJ*, 635, 381
- O'Dwyer, I. J., Chu, Y.-H., Gruendl, R. A., Guerrero, M. A., & Webbink, R. F. 2003, *AJ*, 125, 2239
- Rauch, T., Koeppen, J. & Werner, K. 1994, *A&A*, 286, 543
- Sahai, R., Kastner, J. H., Frank, A., Morris, M., & Blackman, E. G. 2003, *ApJ*, 599, L87
- Sana, H., Rauw, G., & Gosset, E. 2005, in *Massive Stars and High-Energy Emission in OB Associations*, eds. G. Rauw, Y. Nazé, E. Gosset, p.107
- Spitzer, L., 1962, *Physics of Fully Ionized Gases*, (New York: Interscience)
- Tarafdar, S. P., & Apparao, K. M. V. 1988, *ApJ*, 327, 342
- Zweigle, J., Grewing, M., Barnstedt, J., Goelz, M., Gringel, W., Haas, C., Hopfensitz, W., Kappellmann, N., Kraemer, G., Appenzeller, I., Krautter, J., & Mandel, H. 1997, *A&A*, 321, 891